Title

The prebiotic emergence of biological evolution.

Permalink

Journal

Royal Society Open Science, 11(7)

ISSN

2054-5703

Authors

Kocher, Charles

Dill, Kenneth

Publication Date

2024-07-01

DOI

10.1098/rsos.240431

Copyright Information

Peer reviewed

Research

The prebiotic emergence of biological evolution

Charles D. Kocher[1,2] and Ken A. Dill[1,2,3]

[1]Laufer Center for Physical and Quantitative Biology, [2]Department of Physics and Astronomy and [3]Department of Chemistry, Stony Brook University, Stony Brook, NY 11794, USA

CDK, 0000-0001-5032-5186; KAD, 0000-0002-2390-2002

The origin of life must have been preceded by Darwin-like evolutionary dynamics that could propagate it. How did that adaptive dynamics arise? And from what prebiotic molecules? Using evolutionary invasion analysis, we develop a universal framework for describing any origin story for evolutionary dynamics. We find that *cooperative* autocatalysts, i.e. autocatalysts whose per-unit reproductive rate grows as their population increases, have the special property of being able to cross a barrier that separates their initial degradation-dominated state from a growth-dominated state with evolutionary dynamics. For some model parameters, this leap to persistent propagation is likely, not rare. We apply this analysis to the *Foldcat Mechanism*, wherein peptides fold and help catalyse the elongation of each other. Foldcats are found to have cooperative autocatalysis and be capable of emergent evolutionary dynamics.

1. Introduction

It is not known how life arose from prebiotic matter 3.5 billion years ago. It has not been replicated in a laboratory. In the absence of experiments, there is a role for theory and modelling to help generate hypotheses. On the one hand, there have been speculations about 'chicken-or-egg' questions: 'What bio-like molecules might have come first?' Maybe life started as an *RNA World* [1–7]; a *Lipid World* [8–16]; an *Amyloid World* [17–22]; or *Metabolism Came First*, where some biochemical reactions did not require enzyme catalysts [23–27]. Alternatively, the first step towards life could have involved two or more bio-like molecules [28–35].

We reason instead about what *driving forces and dynamics* would have led to sustained bio-like propagation [36–41]. Why was there any tendency at all to create biology? What process might have led polymers (such as lipids, RNA, DNA or proteins) to have specific sequences or assemblies that perform biological functions? While physical and chemical processes tend toward equilibria and degradation according to the Second Law of Thermodynamics, biology is driven by input resources

to survive, evolve and innovate. How did a dead regime dominated by degradation, dilution and transience become a living regime dominated by propagation, evolution and persistence?

Arguably, a Darwin-like evolutionary process must have preceded the origin of life. As a metaphor, computers cannot operate until they have an operating system. A widely accepted definition of living system—due to NASA [42]—is that 'life is a self-sustaining chemical system *capable of Darwinian Evolution*'. The italics are ours, emphasizing the implication that since life cannot be defined in the absence of its adaptation dynamics, then some form of that dynamics must have been operating at or before the origin of life. Life cannot originate until it can propagate. This prebiotic evolution-like process could then act as the driving force that steered prebiotic chemistry toward biology [38,40,43], instead of toward 'asphaltization' or other dead-ends [44–47]. The question of the origin of life then becomes a search for the origin of some *dynamical evolutionary mechanism or process*.

To identify a dynamical origins mechanism requires an analysis at two levels: a macro and micro consideration. At the macro level, we seek the broadest possible statement about what types of fluctuations occurring within an unstable degradation-dominated world could drive a transition to a stable growth-dominated world, independent of any particular microscopic model instantiation of it. At the micro level, we then seek a molecular mechanism that can satisfy this macro criterion for transition to dynamical persistence, and which also has minimal free parameters, is physical, and is prebiotically plausible.

We begin with the macro analysis. We apply a universal framework called 'first invasion' analysis that can be used to probe any proposed origin story for evolutionary dynamics, no matter what its underlying thesis in molecular physics about the origin of life. In short, we are looking for dynamical principles of 'bootstrapping', i.e. of how prebiotic physical and chemical processes dominated by degradation, dilution and decay could transform to stably persistent positive-feedback autocatalysis.

2. First invasion analysis shows three scenarios

The beginnings of some form of evolutionary dynamics must have been when an autocatalyst[1] (or autocatalytic set [48–51]) was able to establish a persistent population of itself. Evolutionary selection would then act on the variation among the characteristics of the autocatalysts and 'remember' the best traits by enhancing them in the population via competition for resources [36,38,52]. Without a persistent population, there is no way for evolutionary dynamics to lock-in its good discoveries and commence its hallmark fitness-ratcheting process.

Suppose an autocatalyst is discovered by a prebiotic chemical process; what would be its fate? Would it grow into a persistent population and establish evolutionary dynamics, or would it decay away before it could do so? Evolutionary invasion analysis [53–57] is a mathematical method for determining whether an individual (the invader), when inserted into a pre-established community, will multiply or die out. The origin of evolution was the 'first successful invasion', the first time where a small population of autocatalysts tried to grow into an environment and succeeded. Therefore, we use an evolutionary invasion analysis to model it, even though the invasion occurs in an environment with no pre-established autocatalysts.

In invasion analysis, the initial population of the invading species is taken to be small enough that it does not perturb the existing community. In a thermodynamics metaphor, this is like a system connected to an infinite thermal bath that it cannot change. In this unperturbing limit, the environment is fixed, so there is only a single dynamical population $A(t)$. In the most general terms, the population will be governed by one differential equation $dA/dt = g(A)$, where the function g depends on the known environmental dynamics. We assume that the timescale of environmental changes is longer than the molecular timescales; while not essential, this simplification allows us to treat $g(A)$ as a constant function (without it, we have $g(A, t)$, where the time dependence is presumed to be known). The invasion analysis limit, which we focus on here, is when $A \to 0$. We discuss various models of the full resource dependence that extend our analysis to larger values of A, as well as the applicability of our invasion analysis approximation, in appendix C, which also outlines the types of population dynamics models that are the starting point for our analysis.

---

[1]An agent A, such as a molecule, is an *autocatalyst* if it accelerates the production of more of itself from some resource materials B, $A + B \to 2A$. For autocatalytic sets, a collection of agents {A} can be used with only small changes to the mathematics. A *cooperative autocatalyst* is, for example, one with reproductive reaction $2A + B \to 3A$, so that the mass-action reaction rate depends on higher powers of A than linear.
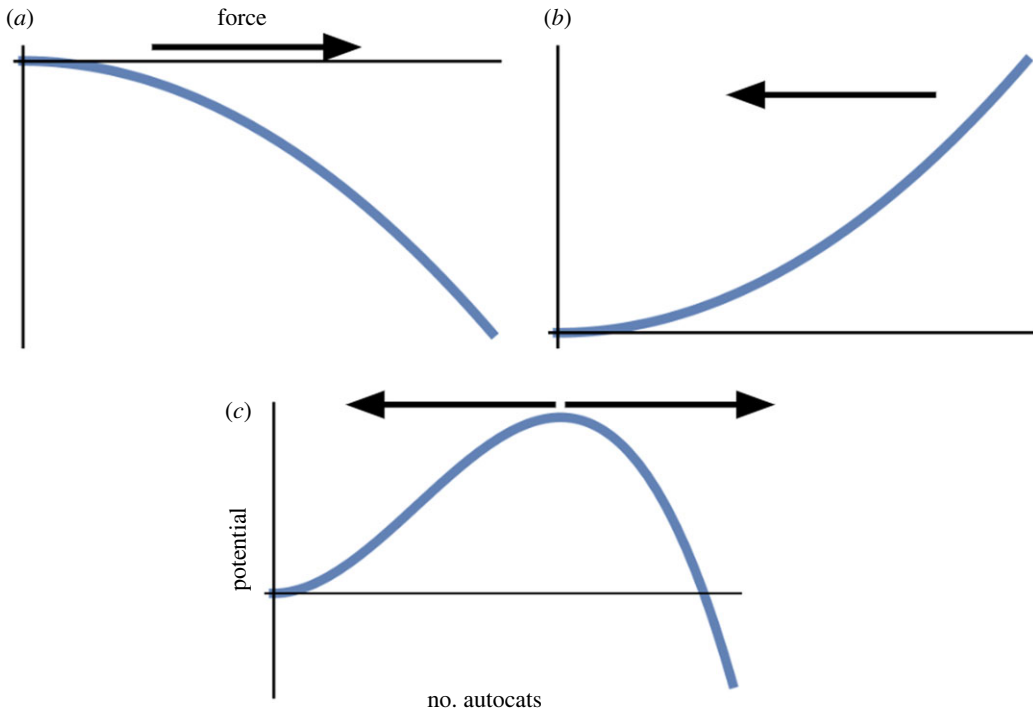
Figure 1. Three possible potential landscapes for invasion. (*a*) Introduced into a *favourable* environment, the invader population grows (until it is limited by the amount of resources; see figure 7). (*b*) Introduced into an *unfavourable* environment, the population is pushed down to zero. (*c*) Degradation at low population; growth at high population. The force changes sign at the potential maximum.

In general, the population $A(t)$ obeys a minimization principle, which we will use to analyse its dynamics. If we define

$$V(A) = -\int_0^A dx\, g(x), \tag{2.1}$$

then $dV(A(t))/dt = (dV/dA)(dA/dt) = -(g(A(t)))^2 \leq 0$ and the population $A(t)$ will tend toward a value that minimizes $V(A)$ while on the path defined by $dA/dt = g(A)$. This potential landscape is a Lyapunov function for the dynamics of the autocatalyst [58]. Stable steady states are minima of V, because at its minima $dV/dA = -g(A) = 0$, and $d^2V/dA^2 = -dg/dA > 0$ guarantees a restoring force $(-dV/dA)$ pointing back to the steady-state value. For a population $A(t)$ to persist and undergo evolution, there only needs to be one such non-zero minimum, where it will sit indefinitely.

In the limit of $A \to 0$, there are only three relevant categories of potential functions, which are visualized in figure 1. Any function $V(A)$ as defined in equation (2.1), when viewed in the small A limit, will fall into one of these three categories. (*a*) *Favourable*. The invader is introduced into a favourable environment and grows until it is limited by resources. The non-equilibrium-driven supply of resources sustains a force $-dV/dA$ (black arrow) that pushes the population of A higher. (*b*) *Unfavourable*. The environment is unfavourable and the population of A dies out. (*c*) *Metastable with a tipping point*. For the small initial population, the invader population does not grow, but for higher populations it does. There is a tipping point that is the transition from a regime of decay to a regime of persistent growth.

These three behaviours are expressed by a general Taylor-expanded version of the ODE for $A(t)$:

$$\frac{dA}{dt} = g(A) \approx (g_1 - D)A + g_2 A^2, \tag{2.2}$$

where g_1 is a growth rate, D is a decay or degradation rate and g_2 is the rate coefficient for a lowest-order nonlinear cooperativity effect. These terms are all that are needed to capture the three fates of the autocatalyst population shown in figure 1. The corresponding potential function of this simple model is

$$V(A) = \frac{(D - g_1)A^2}{2} - \frac{g_2 A^3}{3}. \tag{2.3}$$

Case (*a*) is when $g_2 \geq 0$ and $g_1 > D$, case (*b*) has $g_2 \leq 0$ and $g_1 < D$, and case (*c*) has $g_2 > 0$ and $g_1 < D$. Case (*c*) requires a *cooperative autocatalyst*. Here, we are defining cooperativity in the same way it is defined in

binding polynomials. For example, haemoglobin binds to a second oxygen ligand more tightly when a first oxygen is already bound to it [59–61]. In our situation, cooperativity means the autocatalyst gets better at making itself as its population goes up: the birth rate is $(g_1 + g_2 A)A$, where both constants are positive. Our term cooperativity is a shorthand for positive cooperativity, i.e. where $g_2 > 0$, not negative cooperativity. We note that cooperativity is not a guaranteed property of any autocatalyst that prebiotic chemistry could have discovered: appendix C discusses further when autocatalysts are considered cooperative for the purposes of the invasion analysis approximation and when the approximation holds (i.e. when resource begin to matter again). Case (c) cannot be realized by non-cooperative invaders. Case (b) is non-cooperative ($g_2 = 0$) or negatively cooperative ($g_2 < 0$), and the dynamics of case (a) do not change if the positive cooperativity is removed because the first term of the Taylor expansion is sufficient. We should note here that g_1, g_2 and D are constants because of our assumption that environmental changes are slow; when environmental changes matter, each of these just becomes a (known) function of time, so that the potential landscape that the autocatalyst sees can change. It is only the current potential landscape that determines the autocatalyst's behaviour, since the ODE dynamics are first order in time. We emphasize again that no matter the underlying mechanism or origin of life model of the invading autocatalyst, these three cases can be applied: they are the only possible behaviours.

The deterministic behaviour of case (a) of figure 1 is to give a persistent population of autocatalysts undergoing evolutionary dynamics, while cases (b) and (c) predict that the autocatalysts will die out and there will be no evolution. However, the real dynamics are not deterministic. Cases (a) and (b) do not change when noise is added, but case (c) does. The population $A(t)$ will move around stochastically about its deterministic path. Furthermore, the environment itself is fluctuating. Mathematically, this manifests as fluctuations in the quantities g_1, g_2 and D of equation (2.2). Graphically, this means that the location of the peak of the potential barrier of figure 1c itself can shift. Through these combined motions, case (c) autocatalysts can hop the potential barrier between decay (left side of the barrier) and growth (right side of the barrier). Once it is on the right side, the population will have a sustained driving force toward even higher population levels far away from the barrier, establishing a persistent population that is able to evolve. So, cases (a) and (c) can describe an origin of evolution, while case (b) cannot.

2.1. Using first invasion analysis to probe origin stories

The first invasion analysis described above is completely general, capable of assessing any particular model of origins of life, as we will now argue. It encompasses previous approaches applied to specific models of prebiotic RNA templated polymerization [62,63], a prebiotic disorder-to-order transition [64,65], and other origin of life replicator dynamics models with bistability [66–68]. In particular, we have generalized these models by placing them in a widely applicable ecological framework of the first invasion, distilling out the singular importance of cooperative autocatalysis, and identifying that such dynamics gives rise to evolution's origin. Our main specific application of the first invasion analysis framework will be to the Foldcat Mechanism of peptides in the next section, but in appendix C, we also illustrate its applicability to a simplified model of templated polymerization.

For evolution to emerge from prebiotic chemistry, an autocatalyst must eventually be discovered that is case (a) or case (c). There is no way to begin evolutionary dynamics without discovering the autocatalyst that can evolve (the driving force needs a medium to act on), and the only ways to introduce it are via cases (a) and (c). Origin stories that fit case (a) are of the 'right place at the right time' nature. Prebiotic chemistry would have discovered an autocatalyst in an ideal environment that favoured its growth over decay. The origin story must then explain how that perfect match between environment and autocatalyst was produced using only prebiotic chemistry.

We are interested in mechanisms that are case (c) because these cooperative autocatalysts are able to cross the potential barrier to growth even in unfavourable environments. Moreover, as demonstrated in the specific model of [62,63], this event only needs to happen in one spatially localized place, from which the autocatalysts can diffuse elsewhere into other environments, causing potential barrier crossings wherever they go. Autocatalysts that are non-cooperative, that is, they are case (a) in some places and case (b) in others, cannot do this. Adding more autocatalysts to a case (b) environment cannot flip it into a self-sustaining population; it will always require diffusion from the favourable environment. Diffusion of autocatalysts into a case (c) environment causing a barrier hopping, however, can ignite a self-sustaining population of the autocatalyst that no longer relies on the diffusion of autocatalyst inward. Thus, case (c) has an 'any place at any time' nature. If a cooperative autocatalyst is repeatedly re-introduced into the same case (c) environment, it will *inevitably* hop the potential barrier if given enough time and attempts (depending on the barrier hopping probability and the rate of re-introduction, this amount of time could
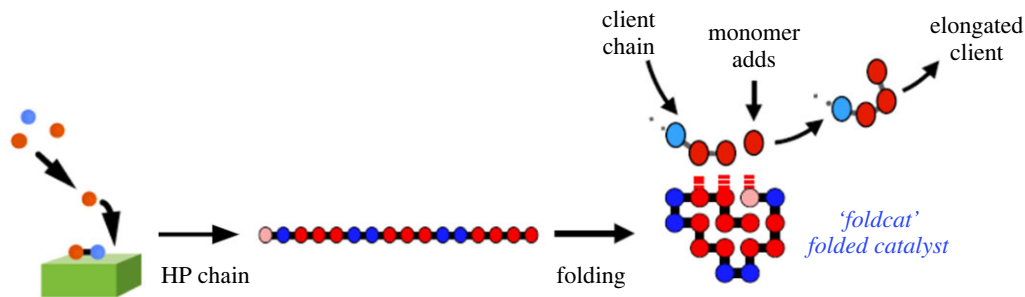
Figure 2. The Foldcat Mechanism. Short peptides of hydrophobic (*H*) and polar (*P*) monomers are synthesized on the 'Founding Rock' catalyst (green). A few long chains fold to stable structures with catalytic-competent surfaces. These can elongate other chains, giving positive feedback of chain-length growth.

be unphysically long, however). Think of it as a biased coin-flip, where the probability of heads is the non-zero probability of hopping the potential barrier. Given enough flips, there will eventually be a heads. Cooperative autocatalysts have a chance, or even a likelihood, of survival even in very poor environments. Cooperativity allows for a much broader range of conditions for the emergence of evolution.

## 3. The Foldcat Mechanism and its emergent evolutionary dynamics

We now give a model at the micro level. The *Foldcat Mechanism*, described previously [36,38,40,69], postulates that the synthesis of random short-chain peptides leads to small populations of longer protein molecules that can both *fold* and *cat*alyse chemical reactions [28,48,70–73]; see figure 2. Short random HP (hydrophobic/polar, referring to the two types of monomers) peptides are synthesized, catalysed at first through some macroscale object, like clays or minerals which, as shorthand, we call *the Founding Rock*. A small fraction of those chains are longer, collapsing into compact conformations with a hydrophobic core. Some of these stable folders have reactive surfaces. Indicated here as having hydrophobic sticky 'landing pads', these chains act as catalysts that grab other peptides and hydrophobic monomers in juxtaposition, accelerating elongation of the client chain (by up to several orders of magnitude according to some estimates [74]). We call chains that fold and catalyse elongation *foldcats*. Here, we analyse the Foldcat Mechanism by invasion analysis to ask if that mechanism admits of parameters that could enable the disorder-to-order bootstrapping transition needed for the origins of evolution.

A key question in the origins of life is what *fitness* might have been before there were cells, in a world that contained only molecules. Through what mechanisms or actions could molecules become self-serving? In the Foldcat Mechanism, the initial *fitness ratcheting* that selects winners from losers is simply molecular *persistence* in the environment. Polymer chain sequences that fold more stably will survive longer. And, chains that are autocatalytic (helping to elongate others) drive to further increase the populations of molecules that are long and autocatalytic.

Another key question at the origin of life is how catalysts could become mobile and programmable. For example, if the Founding Rock was a mineral surface, it would be spatially immobilized and macroscopic. Moreover, it would only catalyse specific reactions, under specific conditions, with no mechanism for tuning its activity. Proteins are biology's catalysts: they are microscopic, freely diffusing, and able to be adjusted (through changes in their sequence) to different environments and functions. The discovery of proteins would be a major event in the origin of life, because catalysis could now move around and be captured in proto-cells [37].

We will show that, as cooperative autocatalysts, foldcats allow for case (c) of the first invasion analysis. They can hop the potential barrier to achieve a persistent population. In doing so, they 'untether' from the Founding Rock's stationary catalysis and are able to sustain their own population as long as they are given an environmental supply of amino acids (discovery of the biological pathways for creating amino acids would be a later development). Mobilizing peptide elongation allows for proteins to spread in their environment, as described for case (c) autocatalysts in the previous section, and begin the process of discovering new catalytic pathways.

There has not been a direct experimental test of the Foldcat Mechanism, but there is experimental evidence for the ideas of folding persistence as the first evolutionary driving force [75–81] and hydrophobic amino acids driving peptide ligation [16,20,82]. Amino acids and short peptides have been generally regarded as existing on the early Earth [28,83–95]. And, reasons have been given for why the most likely first steps entailed proteins, or proteins plus RNA, and not RNA alone [28,31,40,72,96].
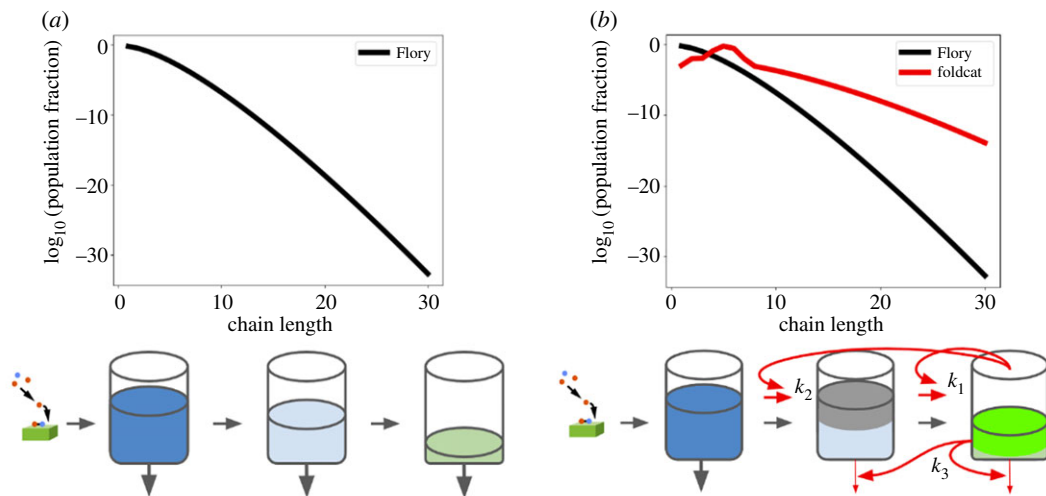
Figure 3. Chain length distributions created by foldcats' cooperativity. (*a*, black) Typical polymerizations produce mostly short chains (shown as bin filling), following a Flory distribution [69,97]. (*b*, red) Foldcats produce more long chains for two reasons: (i) foldcats catalyse elongation of other chains (k_1 and k_2) and (ii) folded chains degrade more slowly because their folded cores are protected from solvent (k_3). For analytical forms, see appendix A.

3.1. Two cooperativities: folding slows degradation; catalysis accelerates elongation

This mechanism entails two contributions to autocatalytic cooperativity: namely, that folded chains degrade slower than unfolded ones because they have protected cores, and that some foldcats serve as catalysts to accelerate the production of longer chains. This mechanism bootstraps to produce longer, more folded, more catalytic molecules. Because of their cooperative feedback, the more foldcats that arise, the higher the rate of producing long, stable, catalytically active chains.

Figure 3 shows the two cooperativity factors of the Foldcat Mechanism. Figure 3*a* is the baseline model powered by the Founding Rock and a supply of monomers: it makes many short chains, fewer medium-length chains, and even fewer long chains. The concentrations of monomers flowing into each chain bin (short, medium, long, folder, foldcat, etc.) can be visualized by the filling of buckets. Each bucket drains into the next bucket on the right, and its chains degrade out of the bottom of the bucket at a fixed rate. The resulting population distribution is plotted above the buckets. Figure 3*b* shows the speed-ups that the Foldcat Mechanism provides beyond the Founding Rock: (i) foldcats (bucket three) elongate chains that are their direct precursors (bucket 2) into foldcats with a rate k_1, (ii) foldcats elongate *the precursors of their precursors* (bucket 1) into the foldcat precursors (bucket 2) with rate k_2 and (iii) the buckets to the right degrade slower because these chains are longer and more folded, with the rate of slowing related to k_3. The first of these three activities is regular autocatalysis; the latter two are cooperative. The result of the foldcat enhancements is the red population distribution, which gives orders of magnitude more long chains when compared to just the Founding Rock's distribution. Analytical forms of both of these population distributions, as well as the example parameters used, are given in appendix A.

3.2. Dynamical model of the Foldcat Mechanism

To keep things simple and focus on how a population of adaptive foldcats could establish itself via the 'first invasion' framework, we do not include chain sequence or chain length information in our first model presented here[2] (although we do include some chain length and sequence information in our models of appendices A and B, to be discussed more later). Our goal is to demonstrate how a foldcat-like autocatalyst with the types of cooperative feedback illustrated in figure 3 gives a region of case (c) metastability behaviour. The basic reactions in our model are that monomer M is supplied at a rate α_M and decays at a rate $d_M M$, while non-foldcat chains r are created at a rate α_r and decay at a

[2]By taking this perspective, we are treating foldcats like an autocatalytic set [48–51]. We are just monitoring the total population of foldcats, of any sequence, averaging over any sequence specificity.

rate $d_r\, r$. Then, we have the elongation reactions, which are catalysed both by the Founding Rock and by our foldcats A: (i) $r + M \rightarrow A$ (non-foldcat is elongated into a foldcat), (ii) $r + M \rightarrow r$ (non-foldcat is elongated and still is not a foldcat), (iii) $A + M \rightarrow A$ (foldcat is elongated and is still a foldcat), and (iv) $A + M \rightarrow r$ (foldcat is elongated and is no longer a foldcat). Elongation reaction i has mass-action rate constant $K_i(A)$, which has a Founding Rock and foldcat contribution. The full set of differential equations describing the Foldcat Mechanism is

$$\left.\begin{array}{l} \dfrac{\mathrm{d}r}{\mathrm{d}t} = \alpha_r - d_r r + K_4(A)AM - K_1(A)rM, \\[2mm] \dfrac{\mathrm{d}M}{\mathrm{d}t} = \alpha_M - [d_M + r(K_1(A) + K_2(A)) + A(K_3(A) + K_4(A))]M, \\[2mm] \dfrac{\mathrm{d}A}{\mathrm{d}t} = K_1(A)rM - K_4(A)AM - DA. \end{array}\right\} \tag{3.1}$$

and

After a few simplification steps (see appendix D for details), equation (3.1) becomes a single equation in $A(t)$:

$$\frac{\mathrm{d}A}{\mathrm{d}t} = \frac{k_1 A}{1 + k_1 A} + \frac{k_1 k_2 A^2}{(1 + k_1 A)(1 + A/A_s)} - A. \tag{3.2}$$

All variables are now dimensionless. The parameters of this mechanism are the non-cooperative reproduction rate k_1, which is the rate at which foldcats elongate non-catalytic chains into foldcats; the cooperative reproduction rate k_2, which is the rate at which foldcats create their direct precursors (a foldcat minus one monomer) from monomers or shorter non-catalytic chains; and an additional free parameter A_s, which is the Michaelis (saturation) constant of the creation of direct precursors from monomers or shorter non-catalytic chains. As described in appendix D, k_1 is a re-defined, dimensionless version of the parameter K_1, and k_2 arises as part of the function α_r. The parameters k_1 and k_2 act as visualized in the bucket metaphor of figure 3. In terms of the first invasion analysis parameters of equation (2.2), Taylor expanding both of the first two terms of equation (3.2) gives $D = 1$ (definition of the dimensionless time parameter, see appendix D), $g_1 = k_1$ and $g_2 = k_1 k_2 - k_1^2$. Surprisingly, even if $k_2 > 0$, there is a region of negative g_2. Even though the nature of the cooperativity may seem straightforward, the range of parameters for which the system is cooperative may be unexpected, and a full analysis like that of appendices C and D is needed.

The corresponding potential function for the Foldcat Mechanism equation (3.2) is

$$V(A) = \frac{A^2}{2} - A - AA_s k_2 - \frac{A_s^3 k_1 k_2 \ln(1 + A/A_s)}{1 - A_s k_1} - \frac{(1 - A_s k_1 + A_s k_2) \ln(1 + k_1 A)}{k_1(A_s k_1 - 1)}. \tag{3.3}$$

Using the three classes of behaviour from figure 1, we can create a phase diagram for foldcats from equation (3.3); see figure 4. The interpretation of this phase diagram is as follows: first, nature discovers foldcats in some environment; then, the values of the parameters k_1, k_2 and A_s are computed for that environment, putting foldcats at one fixed point on the phase diagram; finally, the region in which the point falls determines the foldcats' fate. Each case from figure 1 is represented: one region predicts pure growth (blue), one is pure death (yellow) and one is bistability (green). How quickly the creation of foldcat precursors saturates (magnitude of A_s) determines the extent of the figure 1c metastability region of foldcat discovery.

The simple model of equation (3.2) demonstrates the *cat* part of the Foldcat Mechanism's cooperativity. The other form is the *fold* part. Since our equation (3.2) does not have sequence or chain length information, this type of cooperativity has to be put in by hand (but it arises natively in the more detailed models of appendices A and B). To see the *fold* cooperativity, we should change the decay term in equation (3.2):

$$-A \rightarrow -\left(A - \frac{k_3 A^2}{1 + A^2/B_s^2}\right), \tag{3.4}$$

where k_3 relates to the magnitude of the foldcats' ability to decrease the decay constant, and B_s, like A_s above, characterizes the saturation of the foldcats' degradation fighting effect. The parameter k_3 is visualized in figure 3. Note that the saturating parameters A_s and B_s are necessary: without them, our model would not capture all of the foldcats' possible dynamics. In this sense, the model of foldcats we put forth here is the minimal one (only one additional parameter is needed for each form of cooperativity) that captures the foldcats' type of bootstrapping physics shown in figure 3. In the terms of the invasion analysis parameters of equation (2.2), adding decay cooperativity only changes g_2 to
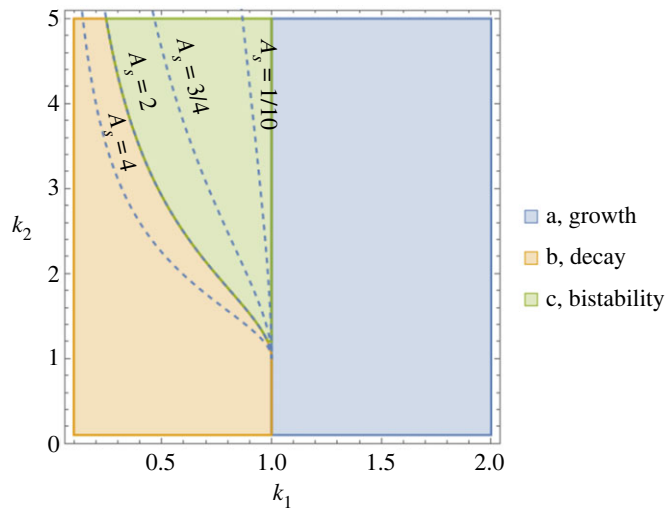
Figure 4. Phase diagram of cases (*a*) growth, (*b*) decay and (*c*) bistability for the Foldcat Mechanism model equations (3.2) and (3.3) when varying the two dimensionless parameters k_1 and k_2. The cases refer to those shown in figure 1. The bistability–decay boundary is shown for various values of the free parameter A_s, which characterizes the concentration of foldcats at which the catalytic cooperativity starts to saturate (see appendix D for details).

$g_2 = k_1 k_2 - k_1^2 + k_3$. Also, k_3 and B_s have a constraint that the term in parentheses in equation (3.4) must always be positive. This requires that $B_s^2 k_3^2 < 4$. The main effect of the decay cooperativity will be to increase the size of the bistability region in figure 4, cutting further into the yellow case (*b*) decay region. The full potential function for foldcats with both cooperative catalysis (k_2) and cooperative chain stability (k_3) is given in appendix D.

3.3. Persistence drives the emergent evolution of the Foldcat Mechanism

To show that our conclusions about the Foldcat Mechanism from equation (3.2) do not change when information about the sequences or chain lengths is added back in, and to obtain information about the time-dependent dynamics of the Foldcat Mechanism, we simulated a modified version of our Foldcat Mechanism model which lumped chains into length and sequence 'bins'. Figure 5 shows the computed time course of this modified model for the parameters given in appendix B. The model predicts a series of epochs: first to appear are short random peptides; later are longer chains, which are enriched in folders and foldcats. Almost all the early production are short useless peptides that degrade back to monomers. It is a dynamical process in which small seedlings of order arise from a sea of disorder, much like modern evolutionary dynamics. Most early molecules are random, short and unproductive. Incrementally advantageous molecules rarely arise within this large sea of options, but when they do further advantages follow from them, and so on, until ultimately a large global advantage has been built up. Throughout the process, the 'persistence' of chains—that is, their fold stability and elongation activity—continually increases. Persistence acts as the fitness for this evolution-like dynamics. Interestingly, we note that the searching behaviour demonstrated in figure 5 is also similar to a previously studied model of protein folding itself as local first, global later [98]. It is a two-step discovery process: first is random search by the Founding Rock, which is then superseded by a driven search by the foldcats.

In this particular simulation, parameters were chosen so that the Foldcat Mechanism was in the case (*a*) region of figure 4. This binned model does have the same cooperativities visualized in figure 3, so cases (*b*) and (*c*) exist as well. In decay scenarios, the light blue 'small foldcat' curve would stay near zero concentration, and the dynamics would stop with the first epoch generated by the Founding Rock search step. However, the Founding Rock would continually rediscover foldcats with some small rate. Since the foldcats are cooperative, if stochastics were taken into account, the small population of foldcats would fluctuate, possibly leading to the explosion in foldcats demonstrated in figure 5 and the later epochs that followed. If the Founding Rock was given enough time to act, the probability of foldcats jumping the potential barrier would approach unity, meaning that the emergence of evolution is a likely property of the Foldcat Mechanism.
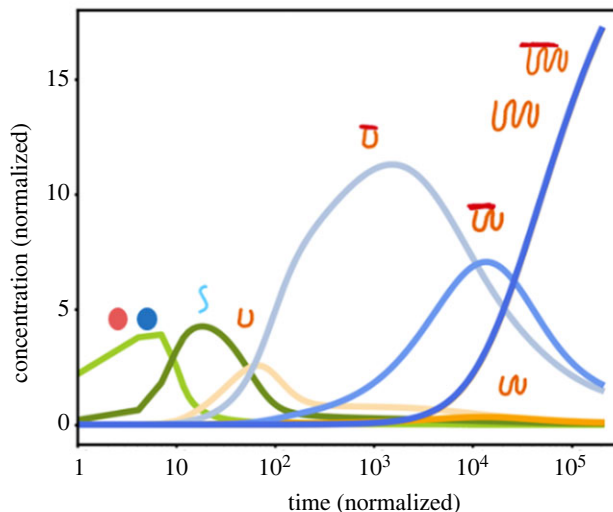
Figure 5. Foldcat Mechanism gives evolutionary dynamics. At first, monomers (light green) are polymerized into short random unfolded chains (dark green), then short folders (light orange) and short foldcats (pale blue), then to longer folders and foldcats (darker blue).

3.4. From persistent foldcats to biology-like inheritance: next steps in the origin of life

We have only addressed a small sliver of how biology arose from chemistry, despite it being among the most mysterious and important open scientific questions. How did persistent autocatalysis arise, leading from polymer chain sequence disorder to order? We now examine the putative steps in this process. (i) Any such mechanism must start from a premise of some pre-existing non-equilibrium environmental process—a driving process that is arguably physico-chemical, is arguably prebiotic, and is capable of producing monomers. Here, we assume amino acid production. (ii) Any such mechanism must assume that the environmental process can 'keep the match lit' long enough for the system to 'keep its own fire going'. That is, the Founding Rock production must be stably persistent until molecular autocatalysts become untethered from the Founding Rock and carry further evolution on their own. We have demonstrated how a population of autocatalytic foldcats could emerge from this non-equilibrium-powered environment by virtue of their cooperativity. (iii) Any mechanism must explain how different monomer sequences have different persistences. In our case, differential persistences come from polymer folding. As argued in the previous subsection, these foldcats would initially be driven towards higher persistence, folding stability and catalytic activity by an evolution-like selection force.

(iv) Any mechanism must set the stage for how and why 'the rest of biology' would follow along either subsequently or concurrently. What would be the further advantage of acquiring cellular encapsulation, coupling proteins with nucleic acids, forming a genetic code, developing lineages and heritability, creating biochemical pathways and networks, and producing its own amino acids and energy storage? In the present picture, once there is a physico-chemical basis for fitness—namely through folding persistence—then any other emergent functionalities can add or subtract value, and fitness now becomes more general. Encapsulation into cells and heritability through a genetic code are huge multipliers of persistence. To summarize these points: once persistence has been established, the next important milestones for life would be fidelity in replication (moving towards biology's system of nucleic acid gene encoding and heredity) and robustness against environmental changes (moving towards cellular encapsulation and biological metabolism/adaptivity).

What can our current model say about faithful replication? In the Foldcat Mechanism as we have studied it here quantitatively, only the functional information of folding and catalysis needs to be passed on for the population to persist. Some sequence information will naturally be passed on, however. The Foldcat Mechanism is inherently biased to preferentially add reactive monomers (ones that stick to landing pads) to growing chains [69]. Such preferences for monomers, or separately for the types of chains that get elongated (potentially even self-preference), constantly work to change the population distribution of foldcat chains, pushing towards more faithfully reproducing foldcats.

However, molecules that function as stores of information have different properties from those that function as molecular machines and catalyse reactions [38,46]. Separation of responsibilities via

specialization allows for better execution of both tasks. Therefore, proteins alone are less 'fit' (or less persistent) than a combined system of proteins and nucleic acids. The simplest argument for how and why biology would develop from a foldcat world is that evolution, via its drive for persistence (e.g. in favouring stabilizing RNA–protein binding [29,99]), was able to act on interacting populations of proteins and ribosomes in order to develop something like a proto-ribosome and a preliminary genetic code [28,100]. The increase in fidelity due to these developments would raise the persistence of the protein chains and turn the persistence fitness ratcheting principle into a form closer to biological evolution's fitness ratcheting.

(v) Finally, we speculate that the development of a specific genetic code, with protein functionalities specified rather precisely, would have been a later development. We envision a disorder-to-order process: at first, there are just vague general autocatalytic sets; only later does it become more precise.

4. Conclusion

The question we have raised in this paper is how prebiotic non-catalytic degradation-prone reactions could have transitioned to autocatalytic persistent growth processes towards biology. Of necessity, this requires explaining the molecular bases of cooperativities and their bootstrapping origins from simpler processes. Our invasion analysis here elucidates the macro constraints that a micro model must satisfy. But simply choosing macro parameters that predict a transition would not be an explanation of origins. An explanation of origins requires a plausible microscopic model that has a physical basis in molecular physics, minimal parameters, and tenable grounding in prebiotic processes. The foldcat hypothesis is found to satisfy these criteria. As random peptides grow longer, they fold, protecting their cores from degradation, and they catalyse the elongation of other chains, accelerating further growth of the population of peptides. It gives a plausible platform for the origins of biological evolution: a persistent population of autocatalytic foldcats feels further evolutionary selection pressures—on its catalytic activity, chain stability and 'reproductive' fidelity—that can continue the development of biology-like life.

Appendix A. Analytical theory of the Foldcat Mechanism

The Foldcat Mechanism has previously been explored through computational simulations [38,69]. Here, we give an analytical approximation to it. Assume we have a monomer u_1—supplied[3] at rate α and decaying at rate Du_1—and that polymerization is able to occur, $u_1 + u_j \rightarrow u_{j+1}$ with rate ku_1u_j. We will not track all of the individual rates of chains breaking apart; instead, we will just assume that there is some rate $d(n)u_n$ that chains completely fall apart (by assuming that chains just decay to nothing, we are getting a lower bound on the number of chains at each level). An ODE model of this reaction system is

$$
\left.
\begin{aligned}
\frac{du_1}{dt} &= \alpha - Du_1 - 2ku_1^2 - \sum_{n=2}^{\infty} ku_nu_1 \\
\frac{du_n}{dt} &= ku_{n-1}u_1 - ku_nu_1 - d(n)u_n.
\end{aligned}
\right\}
\tag{A 1}
$$

and

Solving equation (A 1) is not easy in the general case, but we can use some tricks at steady state. Interpreted the usual way, u_1 would be a function of all of the parameters of the problem: α, D, k, etc.

---

[3]These supply and decay terms help combat the phenomenon of asphaltization [44], where all of the material would get locked up in non-functional compounds, by constantly supplying amino acids to begin the search over sequence space anew. As long as the search continues, there will be a probability of finding interesting chains that can cause a case (c) transition to an evolutionary state.

However, we can instead say that u_1 at steady state is known and solve for the corresponding α using the rate equation for u_1. It is then easy to solve for each u_n recursively:

$$u_n = \frac{ku_1}{ku_1 + d(n)} u_{n-1}. \tag{A2}$$

We can subsequently rewrite u_n non-recursively using a product:

$$u_n = u_1 \prod_{j=2}^{n} \left(\frac{ku_1}{ku_1 + d(j)} \right). \tag{A3}$$

For any set $d(j) > 0$, u_1 is the max of the distribution in equation (A 3), and the population of chains falls off with increasing length. The Flory distribution [97],

$$F_n = a(1-a)^{n-1}, \tag{A4}$$

gives the fraction F_n of chains of length n and is characterized by the parameter a which is the probability that one of a monomer's two connections is the end of the chain it is in. What values of the decay constants $d(j)$ would turn our distribution u_n with a given u_1 into the Flory distribution with a given a and total population U? Setting $U = \sum u_n$, so that we are looking for the form $u_n = U F_n$, we can divide consecutive terms $u_{n+1}/u_n = F_{n+1}/F_n$, to find

$$d(n) = ku_1 \left(\frac{a}{1-a} \right), \tag{A5}$$

a constant. If we plug this result back into the distribution u_n, we find that

$$u_n = u_1 (1-a)^{n-1}. \tag{A6}$$

We see that $U = u_1/a$, as it should. Since the Flory distribution is a special case of our u_n for a given choice of decay constants, we call equation (A 3) the generalized Flory distribution.

If we want to know the fraction of all monomers in chains of length n in the Flory model (equivalent to the mass or weight distribution), we get

$$F_{n,\text{weight}} = na^2 (1-a)^{n-1}. \tag{A7}$$

To find the total amount of monomers in chains of length n in the generalized Flory model, we just multiply in an n:

$$u_{n,\text{weight}} = nu_1 \prod_{j=2}^{n} \left(\frac{ku_1}{ku_1 + d(j)} \right). \tag{A8}$$

A.1. Folding enhances the fraction of large chains

The Flory distribution is exponentially suppressed at large chain length. What about polymers that can fold into stable configurations? For simplicity, we will consider the reaction $u_n \rightleftharpoons f_n$, with folding rate $k_f(n)u_n$ and unfolding rate $k_u(n)f_n$. We will assume that elongation only happens to unfolded chains. Making this assumption, the monomer rate equation does not change, so we find

$$\left. \begin{aligned} \frac{du_n}{dt} &= ku_1(u_{n-1} - u_n) - d(n)u_n + k_u(n)f_n - k_f(n)u_n \\ \frac{df_n}{dt} &= k_f(n)u_n - k_u(n)f_n - d_f(n)f_n. \end{aligned} \right\} \tag{A9}$$

and

To compare to the Flory distribution, we put f_n to steady state:

$$\left. \begin{aligned} \frac{du_n}{dt} &= ku_1(u_{n-1} - u_n) - \left(d(n) + \frac{d_f(n)k_f(n)}{k_u(n) + d_f(n)} \right) u_n \\ f_n &= \frac{k_f(n)}{k_u(n) + d_f(n)} u_n. \end{aligned} \right\} \tag{A10}$$

and

The form of the u_n rate equation is now the same as in the case without folding, where only the decay constants have been modified. The total amount of polymer is

$$p_n = u_n + f_n = \left(1 + \frac{k_f(n)}{k_u(n) + d_f(n)} \right) u_n. \tag{A11}$$

Using the generalized Flory distribution, we can plug in to find

$$p_n = \left(1 + \frac{k_f(n)}{k_u(n) + d_f(n)}\right) u_1 \prod_{j=2}^{n} \frac{ku_1}{ku_1 + d(j) + d_f(j)k_f(j)/(k_u(j) + d_f(j))}. \tag{A 12}$$

We should note that this p_n cannot be directly compared to the generalized Flory distribution because the mapping between u_1 and α is different. The correct comparison would be to look at the two with the same α, not the same u_1. However, in the realistic case where $d_f(n) \ll d(n)$, we can ignore its contribution to the u_n rate equation. The result is that u_n is exactly the generalized Flory distribution result, and that $p_n = (1 + (k_f(n)/k_u(n)))u_n$. Here, the mapping between u_1 and α is the same, so we can directly compare. The enhancement over the generalized Flory distribution depends solely on the ratio of folding to unfolding, which can increase the population of polymer by orders of magnitude.

A.2. Foldcats further beat the Flory distribution

We now introduce foldcats, as in [69]. As we mentioned before, we will not track polymer sequence here. Instead, we will continue to use only length information in our ODEs. Unlike in [69], we are thus not limited in the number of polymers we can track. To deal with the issue of tracking the exponentially growing number of sequences as a function of chain length, Guseva *et al.* introduced a dilution term that kept the total number of chains manageable for their simulation. This dilution completely wiped out the enhancement of folding alone that we reported above after simplifying equation (A12). In our model, we can keep the decay rates general.

Adding foldcats to our model of folding, equation (A 9), is simple. Assume that a fraction $q_{fc}(n)$ of the folded polymers f_n are foldcats. Then, the total number of foldcats is $C = \sum q_{fc}(n)f_n$. If foldcats catalyse the elongation of unfolded chains with a rate $k_c C u_1 u_n$, then we can replace the rate constant k in our equations with the quantity $R = k + k_c C$. Our full model is then

$$\left.\begin{aligned}
\frac{du_1}{dt} &= \alpha - Du_1 - 2Ru_1^2 - \sum_{n=2}^{\infty} Ru_n u_1, \\
\frac{du_n}{dt} &= Ru_1(u_{n-1} - u_n) - d(n)u_n + k_u(n)f_n - k_f(n)u_n \\
\frac{df_n}{dt} &= k_f(n)u_n - k_u(n)f_n - d_f(n)f_n.
\end{aligned}\right\} \tag{A 13}$$

and

We should once again look for the steady-state distribution. We cannot immediately proceed as before, because R now depends on the entire distribution u_n. We no longer get a recursive solution. As before, however, we can recognize that the constants $q_{fc}(n)$ are not what we care about. We can instead swap them out for knowing the level of foldcats C. We have a valid solution for some $q_{fc}(n)$ as long as $C \le \sum f_n$. Just as we traded the supply rate α for the more important parameter u_1, we now trade $q_{fc}(n)$ for the more important C. In doing so, we get the folding solution of equation (A 12), except with k replaced by R. In principle, we could also solve this system of equations self-consistently; we do not do this analysis here.

To compare the foldcat model to the generalized Flory distribution with and without folding, we must simply make sure we have the same α for all three. This is done in figure 6, which shows the fraction of chains at each length for random Founding Rock polymerization only (Flory distribution, black), folding (blue) and foldcats (red). The presence of foldcats allows for many orders of magnitude more long chains in the population. The total number of chains increases in the folding and foldcat cases as well. The parameters used to create this figure, which were just examples chosen to illustrate the foldcat effect, are shown in table 1. These same parameters were used to create figure 3 in the main text.

Appendix B. A binned version of the chain-length-only foldcat model is a two-step process driven by chain persistence

Instead of using the full foldcat model of equation (A 13) to find the time-dependent behaviour of the Foldcat Mechanism, we used a binned model. We tracked ten species: monomers u_1, then chains that do not fold at all u, chains that can fold f, and foldcats c, the three of which could each have
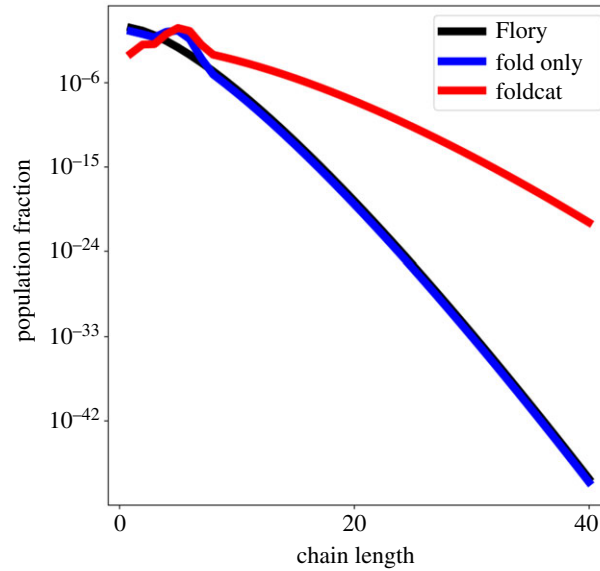
Figure 6. Foldcats enrich long chains by orders of magnitude. Population fraction as a function of chain length for the generalized Flory mechanism (equation (A 8), black curve), the elongation of foldable chains (equation (A 9), blue curve), and the elongation of foldcats (equation (A 13), red curve). The total amount of chains increases as folding and catalysis are added, as well as the fraction of long chains produced. Parameters used for this plot are the same as the ones used in figure 3 in the main text.

Table 1. Parameters used for figures 3 and 6. Units were normalized so that $u_1 = 1$ for the Flory distribution (determines concentration units) and $d(2) = 1$ for the Flory distribution (determines time units). Folding was chosen to peak around $n = 5$, giving the bumps in the red and blue curves of figure 6.

concentration units	$u_1 = 1$
time units	$1/d(2) = 1$
$d(n)$	$d(2) + (n - 2)$
k	1
$d_f(n)$	0
$k_f(n)$	$\exp\left[-(n - 5)^2\right]$
$k_u(n)$	$\exp(-n) + \exp(n - 13)$
k_c	1.8
C	4.145
u_1, foldcat dist.	0.1
D	0.01
implied α	2.72
fraction of folding chains that are foldcats	0.047

lengths short s, medium m, and long l. Our categories were u_1, u_s, u_m, u_l, f_s, f_m, f_l, c_s, c_m and c_l. To compensate for losing specific length information, the elongation reactions were now assumed to be probabilistic. For example, when a u_s is elongated, there is some probability p_{usus} that is stays a u_s, some probability p_{usfs} that it becomes an f_s, some probability p_{uscm} that it becomes a c_m, and so on. Elongation was assumed to be able to change the category to any other either at the same level (e.g. s goes to s) or at the next higher level (e.g. s goes to m and m goes to l). Of course, $\sum_j p_{kj} = 1$ is the normalization condition.

The full model, then, included non-equilibrium supply of monomer, decay of every species back into monomers using an average n_k monomers recovered for decays of chains of length k, joining of two u_1

into a u_s, and the probabilistic elongation of each species that we described above. The ODEs for this binned model are

$$\frac{du_1}{dt} = \alpha - Du_1 + n_s(d_{us}u_s + d_{fs}f_s + d_{cs}c_s) + n_m(d_{um}u_m + d_{fm}f_m + d_{cm}c_m) + n_l(d_{ul}u_l + d_{fl}f_l + d_{cl}c_l)$$
$$- (k_u + k_{uc}c_T)(u_s + u_m + u_l - 2u_1)u_1 - (k_f + k_{fc}c_T)(f_s + f_m + f_l)u_1 - (k_c + k_{cc}c_T)(c_s + c_m + c_l)u_1,$$

$$\frac{du_s}{dt} = (p_{usus} - 1)(k_u + k_{uc}c_T)u_su_1 + p_{fsus}(k_f + k_{fc}c_T)f_su_1 + p_{csus}(k_c + k_{cc}c_T)c_su_1 - d_{us}u_s + (k_u + k_{uc}c_T)u_1^2,$$

$$\frac{du_m}{dt} = p_{usum}(k_u + k_{uc}c_T)u_su_1 + p_{fsum}(k_f + k_{fc}c_T)f_su_1 + p_{csum}(k_c + k_{cc}c_T)c_su_1$$
$$+ (p_{umum} - 1)(k_u + k_{uc}c_T)u_mu_1 + p_{fmum}(k_f + k_{fc}c_T)f_mu_1 + p_{cmum}(k_c + k_{cc}c_T)c_mu_1 - d_{um}u_m,$$

$$\frac{du_l}{dt} = p_{umul}(k_u + k_{uc}c_T)u_mu_1 + p_{fmul}(k_f + k_{fc}c_T)f_mu_1 + p_{cmul}(k_c + k_{cc}c_T)c_mu_1$$
$$+ (p_{ulul} - 1)(k_u + k_{uc}c_T)u_lu_1 + p_{flul}(k_f + k_{fc}c_T)f_lu_1 + p_{clul}(k_c + k_{cc}c_T)c_lu_1 - d_{ul}u_l,$$

$$\frac{df_s}{dt} = p_{usfs}(k_u + k_{uc}c_T)u_su_1 + (p_{fsfs} - 1)(k_f + k_{fc}c_T)f_su_1 + p_{csfs}(k_c + k_{cc}c_T)c_su_1 - d_{fs}f_s,$$

$$\frac{df_m}{dt} = p_{usfm}(k_u + k_{uc}c_T)u_su_1 + p_{fsfm}(k_f + k_{fc}c_T)f_su_1 + p_{csfm}(k_c + k_{cc}c_T)c_su_1$$
$$+ p_{umfm}(k_u + k_{uc}c_T)u_mu_1 + (p_{fmfm} - 1)(k_f + k_{fc}c_T)f_mu_1 + p_{cmfm}(k_c + k_{cc}c_T)c_mu_1 - d_{fm}f_m,$$

$$\frac{df_l}{dt} = p_{umfl}(k_u + k_{uc}c_T)u_mu_1 + p_{fmfl}(k_f + k_{fc}c_T)f_mu_1 + p_{cmfl}(k_c + k_{cc}c_T)c_mu_1$$
$$+ p_{ulfl}(k_u + k_{uc}c_T)u_lu_1 + (p_{flfl} - 1)(k_f + k_{fc}c_T)f_lu_1 + p_{clfl}(k_c + k_{cc}c_T)c_lu_1 - d_{fl}f_l,$$

$$\frac{dc_s}{dt} = p_{uscs}(k_u + k_{uc}c_T)u_su_1 + p_{fscs}(k_f + k_{fc}c_T)f_su_1 + (p_{cscs} - 1)(k_c + k_{cc}c_T)c_su_1 - d_{cs}c_s,$$

$$\frac{dc_m}{dt} = p_{uscm}(k_u + k_{uc}c_T)u_su_1 + p_{fscm}(k_f + k_{fc}c_T)f_su_1 + p_{cscm}(k_c + k_{cc}c_T)c_su_1$$
$$+ p_{umcm}(k_u + k_{uc}c_T)u_mu_1 + p_{fmcm}(k_f + k_{fc}c_T)f_mu_1 + (p_{cmcm} - 1)(k_c + k_{cc}c_T)c_mu_1 - d_{cm}c_m,$$

$$\frac{dc_l}{dt} = p_{umcl}(k_u + k_{uc}c_T)u_mu_1 + p_{fmcl}(k_f + k_{fc}c_T)f_mu_1 + p_{cmcl}(k_c + k_{cc}c_T)c_mu_1$$
$$+ p_{ulcl}(k_u + k_{uc}c_T)u_lu_1 + p_{flcl}(k_f + k_{fc}c_T)f_lu_1 + (p_{clcl} - 1)(k_c + k_{cc}c_T)c_lu_1 - d_{cl}c_l,$$

$$(B\,1)$$

where $c_T = c_s + c_m + c_l$ is the total number of foldcats, k_u is the rate of elongation of a u (similarly for k_f and k_c), and k_{uc} is the rate of catalysed elongation of a u (similarly for k_{fc} and k_{cc}).

There are some heuristics that we used to guide our choices of the values of the (very many) undetermined parameters of this model. Foldcats should be like folders in decay and elongation. It should be easier to elongate an unfoldable chain than a folder or foldcat—k_u or k_{uc} are bigger than their counterparts. On the flip side, unfoldable chains should decay faster. The probability of staying in the same category upon elongation should be highest, while the probability of going to the unfoldable category from either f or c should be small and decrease with chain length. The number of monomers released per chain at each size should be of the order of the previous category's average length plus the inverse of the probability of jumping up a category upon elongation. Our full list of constants used to make figure 5, which demonstrated the persistence-driven two-step nature of the random Founding Rock search followed by the directed foldcat search, is shown in table 2.

Appendix C. Analysing the limits of the invasion analysis approximation and the eventual resource limitation in various models

Our first objective is to see how the invasion analysis that produces figure 1 eventually reaches a stable steady-state population of autocatalysts (autocats) because of resource limitations. The starting point will be the resource competition equations

$$\left.\begin{aligned}\frac{dr}{dt} &= \alpha - d_r r - k(A)Ar \\ \frac{dA}{dt} &= k(A)Ar - DA,\end{aligned}\right\} \qquad (C\,1)$$

and

for one autocat A on one resource r, as developed previously (e.g. [36,38,101,102]). A full resource-dependent population model like the one in equation (C 1) is the most basic starting point for any

15

Table 2. Parameters used for the binned foldcat model. Values were determined using the heuristics described in the text. Units were normalized so that $u_1(0) = 1$ (concentration units) and $u_1(0)/\alpha = 1$ (time units).

α	1	k_f	0.008	p_{usus}	0.864	p_{fsus}	0.01	p_{csus}	0.0055
n_s	15	k_{fc}	0.25	p_{usfs}	0.10	p_{fsfs}	0.718	p_{csfs}	0.01
n_m	50	k_c	0.008	p_{uscs}	0.03	p_{fscs}	0.27	p_{cscs}	0.983
n_l	100	k_{cc}	0.25	p_{usum}	0.005	p_{fsum}	0.0001	p_{csum}	0.0002
k_u	0.02	D	5×10^{-5}	p_{usfm}	0.0007	p_{fsfm}	0.0012	p_{csfm}	0.0003
k_{uc}	1	time units	$u_1(0)/\alpha$	p_{uscm}	0.0003	p_{fscm}	0.0007	p_{cscm}	0.001
p_{umum}	0.718	p_{fmum}	0.001	p_{cmum}	0.0055	p_{ulul}	0.5	p_{clul}	0.0001
p_{umfm}	0.22	p_{fmfm}	0.679	p_{cmfm}	0.01	p_{ulfl}	0.43	p_{clfl}	0.07
p_{umcm}	0.06	p_{fmcm}	0.318	p_{cmcm}	0.983	p_{ulcl}	0.07	p_{clcl}	0.9299
p_{umul}	0.0007	p_{fmul}	0.0001	p_{cmul}	0.0002	p_{flul}	0.001	concentration units	$u_1(0)$
p_{umfl}	0.001	p_{fmfl}	0.001	p_{cmfl}	0.0003	p_{flfl}	0.929		
p_{umcl}	0.0003	p_{fmcl}	0.0009	p_{cmcl}	0.001	p_{flcl}	0.07		

'first invasion' analysis. The resource r is supplied at a rate α, decays with rate constant d_r, and is eaten by the autocats with rate constant $k(A)$. The autocats decay with rate D. Setting the resource to steady state, $dr/dt = 0$, and plugging back into the differential equation for A gives

$$\frac{dA}{dt} = k(A)A\frac{\alpha}{d_r + k(A)A} - DA$$
$$= \frac{(\alpha k(A)/d_r)A}{1 + (k(A)/d_r)A} - DA. \tag{C2}$$

Note that setting the resource to steady state does not contradict the separation of timescales between the system's dynamics and environmental changes that we referred to in the text: we only assume that α and d_r are slowly varying functions of time, not necessarily that they are slow compared to the autocat's dynamics (that is, our assumption was on their derivative, not their value). It is generally expected that, to get the single ODE for $A(t)$ needed for the invasion analysis, resources will be put to their instantaneous steady-state values. We now define $k_1 + k_2 A = (k(A)\alpha/d_r)$ by Taylor expanding $k(A)$. While we expanded $k(A)$ to second order here, there is no reason why k_2 should be non-zero. In each individual model, it must first be argued that the cooperativity exists, and a mechanism for it must be given, before taking $k_2 \neq 0$. This discussion must take place before applying the invasion analysis. Our ODE for the autocat population in this case is

$$\frac{dA}{dt} = \frac{k_1 A + k_2 A^2}{1 + (k_1 A + k_2 A^2)/\alpha} - DA. \tag{C3}$$

We can see that the parameter α, which characterizes the non-equilibrium driving of the system by resource supply, determines when the invasion analysis is valid. When $\alpha \gg k_1 A + k_2 A^2$, we can Taylor expand equation (C3) to find exactly equation (2.2) with $g_1 = k_1$ and $g_2 = k_2 - k_1^2/\alpha$. This is only one example; the actual formula for the parameter that determines when the invasion analysis is valid, or for g_1 and g_2, will depend on the specific mechanism involved (the interplay between the autocatalyst and the resource, as well as the non-equilibrium driving). The Foldcat Mechanism model of equation (3.2) from the main text, for example, has the condition that $A \ll A_s$ and $k_1 A \ll 1$, and we will give further examples shortly. To move to unitless variables, we take time to be measured in units of $1/D$ and concentration to be measured in units of α/D. Our unitless parameters would be $\tilde{A} = DA/\alpha$, $\tilde{k}_1 = k_1/D$, and $\tilde{k}_2 = k_2\alpha/D^2$. Dropping the tildes, we find

$$\frac{dA}{dt} = \frac{k_1 A + k_2 A^2}{1 + k_1 A + k_2 A^2} - A. \tag{C4}$$
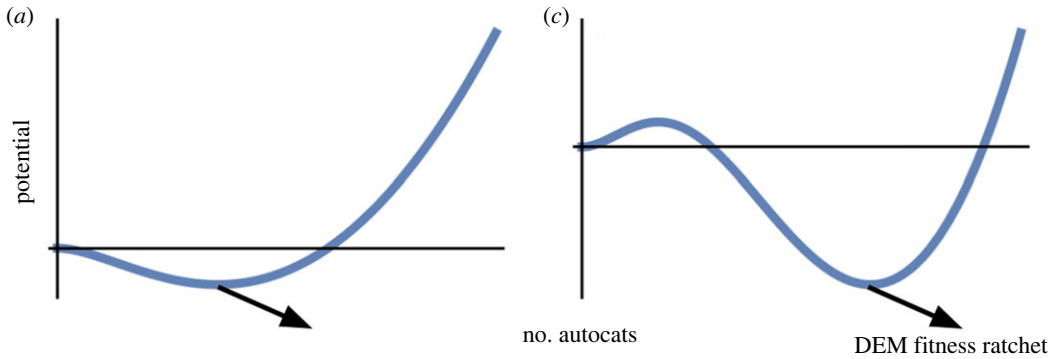
Figure 7. Growth stops when resources are fully subscribed, but then evolution takes over. Situations (*a,c*) as in figure 1, but now with resource limitations included. Figure 1 is the small *A* limit of this one. Each population saturates at a persistent, finite value, at which point evolution acts (through e.g. the Darwinian evolution machine, the DEM [36]) to ratchet up the fitness (black arrow pointing down and to the right).
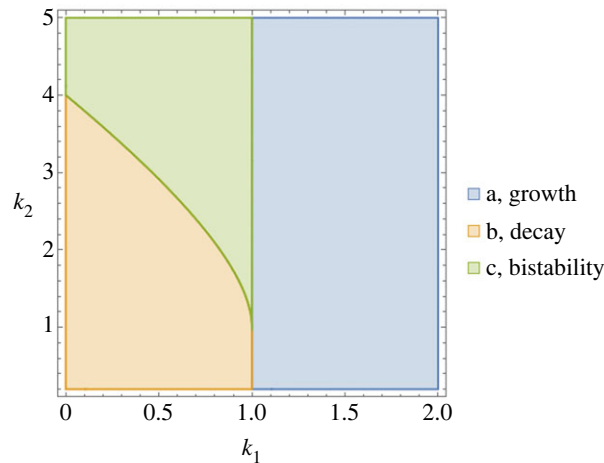
Figure 8. Phase diagram of cases (*a*) growth, (*b*) decay and (*c*) bistability when varying the two dimensionless parameters k_1, which is the rate of non-cooperative reproduction, and k_2, which is the rate of cooperative reproduction, for the potential landscape equation (C 5).

The invasion analysis limit is now $(k_1 A + k_2 A^2) \ll 1$. The corresponding potential landscape is

$$V(A) = \frac{A^2}{2} - A - \frac{2}{\sqrt{4k_2 - k_1^2}} \left(\arctan\left[\frac{k_1}{\sqrt{4k_2 - k_1^2}}\right] - \arctan\left[\frac{k_1 + 2Ak_2}{\sqrt{4k_2 - k_1^2}}\right] \right). \tag{C 5}$$

For cases (a) and (c) as defined in figure 1, we get the full resource-limited dynamics in figure 7. In each case, the population settles to a persistent level when the resource is fully used. When *A* has a persistent population, evolution acts to increase the fitness (move to higher population and lower potential). The invasion analysis figures are the zoomed-in portion near *A* = 0. Case (b) can be considered to be a part of the case (c) plot of figure 7 if the potential barrier does not occur within the invasion analysis regime (our next analysis). The phase diagram for this model is shown in figure 8.

Now that we know when the invasion analysis is valid, we turn to finding when the autocatalyst would be cooperative in the invasion analysis regime. To do this, we need to find the potential barrier maximum of equation (2.2) and compare it to the parameter that determines when the invasion analysis is valid. In general, we will call this parameter *B* (for the previous model, we found $B = \alpha$; for foldcats, $B = \max\{A_s, 1/k_1\}$). If the minimum is greater than *B*, then the autocatalyst is not cooperative: the only way to fluctuate into the funnel of the persistent state is to leave the invasion analysis regime (presumably a very rare event because of the size of fluctuations needed). We will not

plug in explicitly for B; instead, we will only use the parameters defined in the main text. Our starting point is setting equation (2.2) equal to zero. The minimum location is

$$A_0 = \frac{D - g_1}{g_2}. \tag{C6}$$

For our model, then, a cooperative autocat is defined by $A_0 = (D - g_1)/g_2 \lesssim B$, where B is found using the specific mechanism as we illustrated above.

If we are considering a cooperative autocatalytic process with two separate resources put to steady state for the linear and quadratic 'birth' terms, then instead of equation (C4) and (C5), we could use

$$\frac{dA}{dt} = \frac{k_1 A}{1 + A/B} + \frac{k_2 A^2}{1 + A^2/C^2} - DA, \tag{C7}$$

with corresponding potential landscape

$$V(A) = \frac{DA^2}{2} - (k_1 B + k_2 C^2)A + k_2 C^3 \tan^{-1}\left(\frac{A}{C}\right) - k_1 B^2 \ln\left(\frac{B}{B + A}\right). \tag{C8}$$

Now, cooperativity in the invasion analysis regime would be characterized by $A_0 \lesssim B$ and $A_0 \lesssim C$. Both constraints would have to be satisfied for an autocatalyst to be considered case (c).

Finally, we will consider a templated polymerization model. We have templated polymerizers A, monomers M, and non-catalytic polymers r. The reactions are $A + r + M \rightarrow 2\,A + r$ (incorrect copying of an inactive chain to make an active chain), $2\,A + M \rightarrow 3\,A$ (correct copying of an active chain to make another active chain), $A + r + M \rightarrow A + 2\,r$ (correct copying of a non-autocatalytic chain), and $2A + M \rightarrow 2\,A + r$ (incorrect copying of an autocatalytic chain). Note that the second of the reactions, producing $3A$, is the cooperative one (e.g. consider its mass-action rate, which is proportional to A^2). The full ODE model of these reactions, including the non-equilibrium-driven supply terms[4] α_r and α_M, would be

$$\left.\begin{aligned}
\frac{dr}{dt} &= \alpha_r - d_r r + k_1 A r M + k_4 A^2 M, \\
\frac{dM}{dt} &= \alpha_M - d_M M - (k_1 + k_2) A r M - (k_3 + k_4) A^2 M \\
\frac{dA}{dt} &= k_2 A r M + k_3 A^2 M - DA,
\end{aligned}\right\} \tag{C9}$$

and

where k_1 is the mass-action rate of faithful copying of an r, k_2 is the rate of unfaithful copying of an r, and k_3 and k_4 are the rates of faithful and unfaithful copying of an A, respectively. By assuming M and r attain their steady states with $A = 0$, we can find that the maximum of the potential barrier for the templated polymerizers would appear at

$$A_0^{TP} = \frac{d_r d_M D - k_2 \alpha_r \alpha_M}{k_3 \alpha_M d_r}. \tag{C10}$$

We could proceed as previously, putting the resources r and M to steady state then comparing A_0^{TP} to the concentration parameter that determines when we can Taylor expand the rate equation for A, but the expressions for r_{SS} and M_{SS} are unwieldy (although we should note that if r is presumed to be constant, and the processes k_1 and k_4 are ignored, then equation (C9) reduces to equation (C4)). Instead, we will approximate. We note that the invasion analysis approximation is when $r \approx \alpha_r/d_r$ and $M \approx \alpha_M/d_M$. That is, only the zeroth-order term of the Taylor expansion of r and M in powers of A contributes. Explicitly, this expansion is $r = \alpha_r/d_r + g_r A$ and $M = \alpha_M/d_M + g_M A$ for some constants g_r and g_M. The invasion analysis approximation holds at the potential barrier maximum if $g_r A_0^{TP} d_r/\alpha_r \lesssim 1$ and $g_M A_0^{TP} d_M/\alpha_M \lesssim 1$. Setting the first two ODEs of equation (C9) to steady state using only terms up to linear order in A gives

$$\left.\begin{aligned}
g_r &= \frac{k_1 \alpha_r \alpha_M}{d_r^2 d_M} \\
g_M &= \frac{(k_1 + k_2) \alpha_r \alpha_M}{d_M^2 d_r},
\end{aligned}\right\} \tag{C11}$$

and

---

[4]In general, α_r should be a complicated function of M. We will ignore that. It actually does not affect the invasion analysis that we do here, since M is approximately constant anyway. We assume the use of monomers to make r is rolled into the decay term d_M.

so that the conditions for a cooperative autocat are

$$
\left.\begin{array}{c}
\dfrac{k_1 \alpha_M A_0^{TP}}{d_r d_M} \lesssim 1 \\[2ex]
\dfrac{(k_1 + k_2)\alpha_r A_0^{TP}}{d_r d_M} \lesssim 1.
\end{array}\right\} \tag{C 12}
$$

and

Appendix D. The foldcat-like cooperativity model

First, we should see why foldcat catalysis is actually cooperative in the first place. For templated polymerizers, it is easy to see that the reaction $2A + M \rightarrow 3A$ has a mass-action rate proportional to A^2, giving the cooperativity. On the other hand, foldcats catalyse elongation reactions. One such reaction would be a foldcat A taking a non-catalytic chain r and adding a monomer M to it to make a resultant chain that is another foldcat: $A + r + M \rightarrow 2A$. Alternatively, a foldcat can elongate a foldcat and keep it as a foldcat, $2A + M \rightarrow 2A$. In the latter reaction, there is no net change in the number of foldcats. In the former, one foldcat is added, but the mass-action rate of reaction is only proportional to Ar. At first glance, then, it seems like foldcats are not cooperative, since there is no factor of A^2. However, foldcats also catalyse the formation of r from only M. Thus, the amount of precursor r should be a function of A; Taylor expanding $r(A) = r_0 + r_1 A$ gives the extra factor of A necessary for cooperativity in foldcat dynamics.

We will now write down a full toy model of the Foldcat Mechanism just as we did for templated polymerization in the previous appendix section. We will then simplify this model to the form that we worked with in the main text. Our basic reactions, which we will simplify further below, are that monomer M is non-equilibrium supplied at a rate α_M and decays at a rate $d_M M$, while non-catalytic chains r are created at a rate α_r and decay at a rate $d_r r$. Then, we have the elongation reactions, which are catalysed by the Founding Rock and by our foldcats A: (1) $r + M \rightarrow A$ (non-foldcat is elongated into a foldcat), (2) $r + M \rightarrow r$ (non-foldcat elongated and still is not a foldcat), (3) $A + M \rightarrow A$ (foldcat is elongated and is still a foldcat) and (4) $A + M \rightarrow r$ (foldcat is elongated and is no longer a foldcat). Elongation reaction i has mass-action rate constant $K_i(A)$. The full ODE model is

$$
\left.\begin{array}{l}
\dfrac{dr}{dt} = \alpha_r - d_r r + K_4(A)AM - K_1(A)rM, \\[2ex]
\dfrac{dM}{dt} = \alpha_M - [d_M + r(K_1(A) + K_2(A)) + A(K_3(A) + K_4(A))]M \\[2ex]
\dfrac{dA}{dt} = K_1(A)rM - K_4(A)AM - DA.
\end{array}\right\} \tag{D 1}
$$

and

Foldcats also cause the creation of chains r from just monomer, so $\alpha_r = \alpha_r(A, M)$. This observation[5] is key for the cooperativity of foldcats. If we now suppose that $M = M_0/(1 + A/A_s)$ has a saturating form as the resource from equation (C 2) does, where the quantity A_s determines when the foldcats' creation of r can go no faster and M_0 is the amount of monomer when no foldcats are present, then we can make further progress. We will use the linear approximation for the rate of creation of r: $\alpha_r(A, M) = \alpha + \alpha_2 AM/M_0 = \alpha + \alpha_2 A/(1 + A/A_s)$.

To keep things simple, we only want to use this form of M in the function $\alpha_r(A, M)$; we do not want to use it when it is multiplying a rate of elongation. That is, we want the zeroth-order expansion $M \approx M_0$ to be sufficient for the terms with K_i in our model. This simplification requires that the first-order corrections (e.g. $M_0 K_1(A)Ar/A_s$ for the K_1 term) to the elongation rates defined by the K_i are much smaller than the first-order correction to α_r. Said differently, we are assuming that our main process is the creation of r from M via the rate α_r, and that the elongation reactions are themselves already first-order corrections to this reaction. This assumption is reasonable physically because we are only interested in the region when foldcats are first introduced, so that their effect is small. Making these approximations, we find the reactions

$$
\left.\begin{array}{l}
\dfrac{dr}{dt} = \alpha + \dfrac{\alpha_2 A}{1 + A/A_s} - d_r r + K_4'(A)A - K_1'(A)r \\[2ex]
\dfrac{dA}{dt} = K_1'(A)r - K_4'(A)A - DA,
\end{array}\right\} \tag{D 2}
$$

and

---

[5]In a more detailed model that kept track of sequence as well, the important point is that foldcats create sequences that can be elongated into foldcats, not just that foldcats create dimers from monomer as here.

where we have absorbed the constant amount of monomer M_0 into the definitions of the functions $K_i'(A) = M_0 K_i(A)$. We are most concerned with foldcat untethering from the Founding Rock, so we make some further assumptions. Founding Rock terms in $K_i'(A)$ would be constants, while foldcat terms are, in the first approximation, proportional to A. We drop the constant terms. Further, we assume the reaction (4) that elongates foldcats into non-foldcats is very rare, so we drop it altogether.[6] Upon defining $\alpha_2 = \alpha k_2$, we find the ODEs

$$\left.\begin{aligned} \frac{\mathrm{d}r}{\mathrm{d}t} &= \alpha + \frac{\alpha k_2 A}{1 + A/A_s} - d_r r - K_1' A r \\ \frac{\mathrm{d}A}{\mathrm{d}t} &= K_1' A r - DA. \end{aligned}\right\} \tag{D3}$$

and

Setting the non-catalytic chains r to steady state finally gives the dynamical equation for the foldcats:

$$\frac{\mathrm{d}A}{\mathrm{d}t} = \left(\alpha + \frac{\alpha k_2 A}{1 + A/A_s}\right) \frac{K_1' A}{d_r + K_1' A} - DA. \tag{D4}$$

Further simplification is now possible by redefining $k_1 = K_1'/d_r$, which eliminates the parameter d_r, and by choosing units in which $\alpha = 1$ and $D = 1$. This choice is equivalent to measuring time in units of $1/D$ and measuring concentration in units of α/D. Finally, we are left with the rate equation considered in the main text in terms of only dimensionless variables:

$$\frac{\mathrm{d}A}{\mathrm{d}t} = \frac{k_1 A}{1 + k_1 A} + \frac{k_1 k_2 A^2}{(1 + k_1 A)(1 + A/A_s)} - A. \tag{D5}$$

The parameters of our model are k_1, which is related to the rate at which foldcats elongate non-catalytic chains into foldcats; k_2, which is related to the rate at which foldcats create their direct precursors (a foldcat minus one monomer) from monomers or shorter non-catalytic chains; and A_s, which is the Michaelis constant of the creation of direct precursors from monomers or shorter non-catalytic chains.

To include the cooperative effects of increased chain stability, we can change the decay term as indicated in the main text, slowing the decay by a new term that has saturation constant B_s. The full ODE is

$$\frac{\mathrm{d}A}{\mathrm{d}t} = \frac{k_1 A}{1 + k_1 A} + \frac{k_1 k_2 A^2}{(1 + k_1 A)(1 + A/A_s)} - \left(A - \frac{k_3 A^2}{1 + A^2/B_s^2}\right), \tag{D6}$$

where the term in parentheses is constrained to be positive (this requirement puts a constraint on k_3 and B_s, namely that $B_s^2 k_3^2 < 4$). The full potential function for foldcats with both types of cooperativity is

$$\begin{aligned} V(A) = {} & \frac{A^2}{2} - A - A A_s k_2 - \frac{A_s^3 k_1 k_2 \ln(1 + A/A_s)}{1 - A_s k_1} \\ & - \frac{(1 - A_s k_1 + A_s k_2)\ln(1 + k_1 A)}{k_1(A_s k_1 - 1)} - A B_s^2 k_3 + B_s^3 k_3 \arctan\left(\frac{A}{B_s}\right). \end{aligned} \tag{D7}$$

References

1. Gilbert W. 1986 Origin of life: the RNA world. *Nature* **319**, 618–618. (doi:10.1038/319618a0)
2. Joyce GF, Szostak JW. 2018 Protocells and RNA self-replication. *Cold Spring Harb. Perspect. Biol.* **10**, a034801. (doi:10.1101/cshperspect.a034801)
3. Atkins JF, Gesteland RF, Cech T. 2011 *RNA worlds: from life's origins to diversity in gene regulation*. Cold Spring Harbor, NY: Cold Spring Harbor Laboratory Press.
4. Reader JS, Joyce GF. 2002 A ribozyme composed of only two different nucleotides. *Nature* **420**, 841–844. (doi:10.1038/nature01185)
5. Horning DP, Joyce GF. 2016 Amplification of RNA by an RNA polymerase ribozyme. *Proc. Natl Acad. Sci. USA* **113**, 9786–9791. (doi:10.1073/pnas.1610103113)
6. Wochner A, Attwater J, Coulson A, Holliger P. 2011 Ribozyme-catalyzed transcription of an active ribozyme. *Science* **332**, 209–212. (doi:10.1126/science.1200752)
7. Johnston WK, Unrau PJ, Lawrence MS, Glasner ME, Bartel DP. 2001 RNA-catalyzed RNA polymerization: accurate and general RNA-templated primer extension. *Science* **292**, 1319–1325. (doi:10.1126/science.1060786)
8. Segré D, Ben-Eli D, Deamer DW, Lancet D. 2001 The lipid world. *Orig. Life Evol. Biosph.* **31**, 119–145.
9. Damer B, Deamer D. 2020 The hot spring hypothesis for an origin of life. *Astrobiology* **20**, 429–452. (doi:10.1089/ast.2019.2045)
10. Deamer DW. 1994 *Origins of life: the central concepts*. Boston, MA: Jones and Bartlett Publishers.
11. Lancet D, Zidovetzki R, Markovitch O. 2018 Systems protobiology: origin of life in lipid catalytic networks. *J. R. Soc. Interface* **15**, 20180159. (doi:10.1098/rsif.2018.0159)
12. Armstrong DL, Lancet D, Zidovetzki R. 2018 Replication of simulated prebiotic amphiphilic vesicles in a finite environment exhibits complex behavior that includes high progeny variability and competition. *Astrobiology* **18**, 419–430. (doi:10.1089/ast.2016.1615)

[6]The derivation would have been cleaner if we had started by dropping the Founding Rock's contribution and the foldcat elongates to a non-foldcat reaction; however, we kept them in until this stage to show exactly when it becomes simplest to neglect them, instead of inexplicably neglecting them from the outset.

13. Segré D, Ben-Eli D, Lancet D. 2000 Prebiotic evolution of amphiphilic assemblies far from equilibrium: from compositional information to sequence-based biopolymers. In *Bioastronomy 99*, vol. 213 (eds G Lamarchand, K Meech), pp. 373–378. Orem, UT: Astronomical Society of the Pacific.

14. Rufo CM, Moroz YS, Moroz OV, Stöhr J, Smith TA, Hu X, DeGrado WF, Korendovych IV. 2014 Short peptides self-assemble to produce catalytic amyloids. *Nat. Chem.* **6**, 303–309. (doi:10.1038/nchem.1894)

15. Greenwald J, Friedmann MP, Riek R. 2016 Amyloid aggregates arise from amino acid condensations under prebiotic conditions. *Angew. Chem.* **128**, 11 781–11 785. (doi:10.1002/ange.201605321)

16. Takahashi Y, Mihara H. 2004 Construction of a chemically and conformationally self-replicating system of amyloid-like fibrils. *Bioorg. Med. Chem.* **12**, 693–699. (doi:10.1016/j.bmc.2003.11.022)

17. Maury CPJ. 2018 Amyloid and the origin of life: self-replicating catalytic amyloids as prebiotic informational and protometabolic entities. *Cell. Mol. Life Sci.* **75**, 1499–1507. (doi:10.1007/s00018-018-2797-9)

18. Maury CPJ. 2015 Origin of life. Primordial genetics: information transfer in a pre-RNA world based on self-replicating beta-sheet amyloid conformers. *J. Theor. Biol.* **382**, 292–297. (doi:10.1016/j.jtbi.2015.07.008)

19. Maury CPJ. 2009 Self-propagating β-sheet polypeptide structures as prebiotic informational molecular entities: the amyloid world. *Orig. Life Evol. Biosph.* **39**, 141–150. (doi:10.1007/s11084-009-9165-6)

20. Rout SK, Friedmann MP, Riek R, Greenwald J. 2018 A prebiotic template-directed peptide synthesis based on amyloids. *Nat. Commun.* **9**, 234. (doi:10.1038/s41467-017-02742-3)

21. Carny O, Gazit E. 2005 A model for the role of short self-assembled peptides in the very early stages of the origin of life. *FASEB J.* **19**, 1051–1055. (doi:10.1096/fj.04-3256hyp)

22. Greenwald J, Riek R. 2010 Biology of amyloid: structure, function, and regulation. *Structure* **18**, 1244–1260. (doi:10.1016/j.str.2010.08.009)

23. Muchowska KB, Varma SJ, Moran J. 2020 Nonenzymatic metabolic reactions and life's origins. *Chem. Rev.* **120**, 7708–7744. (doi:10.1021/acs.chemrev.0c00191)

24. Wachtershauser G. 1988 Before enzymes and templates: theory of surface metabolism. *Microbiol. Rev.* **52**, 452–484.

25. Shapiro R. 2006 Small molecule interactions were central to the origin of life. *Q. Rev. Biol.* **81**, 105–126. (doi:10.1086/506024)

26. Jordan SF et al. 2021 Spontaneous assembly of redox-active iron-sulfur clusters at low concentrations of cysteine. *Nat. Commun.* **12**, 5925. (doi:10.1038/s41467-021-26158-2)

27. Cody GD. 2004 Transition metal sulfides and the origins of metabolism. *Annu. Rev. Earth Planet. Sci.* **32**, 569–599. (doi:10.1146/annurev.earth.32.101802.120225)

28. Fried SD, Fujishima K, Makarov M, Cherepashuk I, Hlouchova K. 2022 Peptides before and during the nucleotide world: an origins story emphasizing cooperation between proteins and nucleic acids. *J. R. Soc. Interface* **19**, 20210641. (doi:10.1098/rsif.2021.0641)

29. Carter CW, Kraut J. 1974 A proposed model for interaction of polypeptides with RNA. *Proc. Natl Acad. Sci. USA* **71**, 283–287. (doi:10.1073/pnas.71.2.283)

30. Giacobelli VG, Fujishima K, Lepšík M, Tretyachenko V, Kadavá T, Makarov M, Bednárová L, Novák P, Hlouchová K. 2022 In vitro evolution reveals noncationic protein–RNA interaction mediated by metal ions. *Mol. Biol. Evol.* **39**, msac032. (doi:10.1093/molbev/msac032)

31. Wills PR, Carter CW. 2018 Insuperable problems of the genetic code initially emerging in an RNA world. *Biosystems* **164**, 155–166. (doi:10.1016/j.biosystems.2017.09.006)

32. Alva V, Söding J, Lupas AN. 2015 A vocabulary of ancient peptides at the origin of folded proteins. *eLife* **4**, e09410. (doi:10.7554/eLife.09410)

33. Dale T. 2006 Protein and nucleic acid together: a mechanism for the emergence of biological selection. *J. Theor. Biol.* **240**, 337–342. (doi:10.1016/j.jtbi.2005.09.027)

34. Adamala K, Szostak JW. 2013 Nonenzymatic template-directed RNA synthesis inside model protocells. *Science* **342**, 1098–1100. (doi:10.1126/science.1241888)

35. Pressman A, Blanco C, Chen IA. 2015 The RNA world as a model system to study the origin of life. *Curr. Biol.* **25**, R953–R963. (doi:10.1016/j.cub.2015.06.016)

36. Kocher CD, Dill KA. 2023 Darwinian evolution as a dynamical principle. *Proc. Natl Acad. Sci. USA* **120**, e2218390120. (doi:10.1073/pnas.2218390120)

37. Kocher C, Agozzino L, Dill K. 2021 Nanoscale catalyst chemotaxis can drive the assembly of functional pathways. *J. Phys. Chem. B* **125**, 8781–8786. (doi:10.1021/acs.jpcb.1c04498)

38. Kocher C, Dill KA. 2023 Origins of life: first came evolutionary dynamics. *QRB Discov.* **4**, e4. (doi:10.1017/qrd.2023.2)

39. Pross A. 2003 The driving force for life's emergence: kinetic and thermodynamic considerations. *J. Theor. Biol.* **220**, 393–406. (doi:10.1006/jtbi.2003.3178)

40. Dill KA, Agozzino L. 2021 Driving forces in the origins of life. *Open Biol.* **11**, 200324. (doi:10.1098/rsob.200324)

41. Pross A. 2016 *What is life? How chemistry becomes biology*. Oxford, UK: Oxford University Press.

42. Joyce GF, Deamer DW, Fleischaker G. 1994 Foreword. In *Origins of life: the central concepts*. Boston, MA: Jones and Bartlett Publishers.

43. Pross A. 2011 Toward a general theory of evolution: extending Darwinian theory to inanimate matter. *J. Syst. Chem.* **2**, 1. (doi:10.1186/1759-2208-2-1)

44. Benner SA, Kim H-J, Carrigan MA. 2012 Asphalt, water, and the prebiotic synthesis of ribose, ribonucleosides, and RNA. *Acc. Chem. Res.* **45**, 2025–2034. (doi:10.1021/ar200332w)

45. Benner SA. 2014 Paradoxes in the origin of life. *Orig. Life Evol. Biosph.* **44**, 339–343. (doi:10.1007/s11084-014-9379-0)

46. Neveu M, Kim H-J, Benner SA. 2013 The 'strong' RNA world hypothesis: fifty years old. *Astrobiology* **13**, 391–403. (doi:10.1089/ast.2012.0868)

47. Camprubí E, de Leeuw JW, House CH, Raulin F, Russell MJ, Spang A, Tirumalai MR, Westall F. 2019 The emergence of life. *Space Sci. Rev.* **215**, 56.

48. Kauffman SA. 1986 Autocatalytic sets of proteins. *J. Theor. Biol.* **119**, 1–24. (doi:10.1016/S0022-5193(86)80047-9)

49. Hordijk W. 2019 A history of autocatalytic sets. *Biol. Theory* **14**, 224–246. (doi:10.1007/s13752-019-00330-w)

50. Kauffman SA. 1971 Cellular homeostasis, epigenesis and replication in randomly aggregated macromolecular systems. *J. Cybern.* **1**, 71–96. (doi:10.1080/01969727108545830)

51. Hordijk W, Steel M. 2014 Conditions for evolvability of autocatalytic sets: a formal example and analysis. *Orig. Life Evol. Biosph.* **44**, 111–124. (doi:10.1007/s11084-014-9374-5)

52. Kirschner MW, Gerhart JC. 2005 *The plausibility of life: resolving Darwin's dilemma*. New Haven, CT: Yale University Press.

53. Barabás G, D'Andrea R, Maccracken Stump S. 2018 Chesson's coexistence theory. *Ecol. Monogr.* **88**, 277–303.

54. Turelli M. 1978 Does environmental variability limit niche overlap?. *Proc. Natl Acad. Sci. USA* **75**, 5085–5089. (doi:10.1073/pnas.75.10.5085)

55. Chesson PL, Ellner S. 1989 Invasibility and stochastic boundedness in monotonic competition models. *J. Math. Biol.* **27**, 117–138. (doi:10.1007/BF00276099)

56. Gard TC. 1984 Persistence in stochastic food web models. *Bull. Math. Biol.* **46**, 357–370. (doi:10.1016/S0092-8240(84)80044-0)

57. Schreiber SJ, Benaïm M, Atchadé KAS. 2011 Persistence in fluctuating environments. *J. Math. Biol.* **62**, 655–683. (doi:10.1007/s00285-010-0349-5)

58. Yang Y-J, Cheng Y-C. 2021 Potentials of continuous Markov processes and random perturbations. *J. Phys. A: Math. Theor.* **54**, 195001. (doi:10.1088/1751-8121/abef80)

59. Vivian Hill A. 1910 The possible effects of the aggregation of the molecules of hemoglobin on its dissociation curves. *J. Physiol.* **40**, iv–vii.

60. Adair GS, Bock AV, Field Jr H. 1925 The hemoglobin system: VI. The oxygen dissociation curve of hemoglobin. *J. Biol. Chem.* **63**, 529–545. (doi:10.1016/S0021-9258(18)85018-9)

61. Abeliovich H. 2005 An empirical extremum principle for the Hill coefficient in ligand-protein interactions showing negative cooperativity. *Biophys. J.* **89**, 76–79. (doi:10.1529/biophysj.105.060194)

62. Wu M, Higgs PG. 2012 The origin of life is a spatially localized stochastic transition. *Biol. Direct* **7**, 42. (doi:10.1186/1745-6150-7-42)

63. Shay JA, Huynh C, Higgs PG. 2015 The origin and spread of a cooperative replicase in a prebiotic chemical system. *J. Theor. Biol.* **364**, 249–259. (doi:10.1016/j.jtbi.2014.09.019)

64. Dyson FJ. 1982 A model for the origin of life. *J. Mol. Evol.* **18**, 344–350. (doi:10.1007/BF01733901)

65. Dyson F. 1999 *Origins of life*. Cambridge, UK: Cambridge University Press.

66. Ohtsuki H, Nowak MA. 2009 Prelife catalysts and replicators. *Proc. R. Soc. B* **276**, 3783–3790. (doi:10.1098/rspb.2009.1136)

67. Manapat M, Ohtsuki H, Bürger R, Nowak MA. 2009 Originator dynamics. *J. Theor. Biol.* **256**, 586–595. (doi:10.1016/j.jtbi.2008.10.006)

68. Eigen M, McCaskill J, Schuster P. 1988 Molecular quasi-species. *J. Phys. Chem.* **92**, 6881–6891. (doi:10.1021/j100335a010)

69. Guseva E, Zuckermann RN, Dill KA. 2017 Foldamer hypothesis for the growth and sequence differentiation of prebiotic polymers. *Proc. Natl Acad. Sci. USA* **114**, E7460–E7468. (doi:10.1073/pnas.1620191114)

70. Matsuo M, Kurihara K. 2021 Proliferating coacervate droplets as the missing link between chemistry and biology in the origins of life. *Nat. Commun.* **12**, 5487. (doi:10.1038/s41467-021-25530-6)

71. Ikehara K. 2014 [GADV]-protein world hypothesis on the origin of life. *Orig. Life Evol. Biosph.* **44**, 299–302. (doi:10.1007/s11084-014-9383-4)

72. Frenkel-Pinter M, Samanta M, Ashkenasy G, Leman LJ. 2020 Prebiotic peptides: molecular hubs in the origin of life. *Chem. Rev.* **120**, 4707–4765. (doi:10.1021/acs.chemrev.9b00664)

73. Lee DH, Granja JR, Martinez JA, Severin K, Reza Ghadiri M. 1996 A self-replicating peptide. *Nature* **382**, 525–528. (doi:10.1038/382525a0)

74. Menger FM, Nome F. 2019 Interaction vs preorganization in enzyme catalysis. A dispute that calls for resolution. *ACS Chem. Biol.* **14**, 1386–1392. (doi:10.1021/acschembio.8b01029)

75. Shibue R, Sasamoto T, Shimada M, Zhang B, Yamagishi A, Akanuma S. 2018 Comprehensive reduction of amino acid set in a protein suggests the importance of prebiotic amino acids for stable proteins. *Sci. Rep.* **8**, 1227. (doi:10.1038/s41598-018-19561-1)

76. Makarov M *et al.* 2023 Early selection of the amino acid alphabet was adaptively shaped by biophysical constraints of foldability. *J. Am. Chem. Soc.* **145**, 5320–5329. (doi:10.1021/jacs.2c12987)

77. Makarov M *et al.* 2021 Enzyme catalysis prior to aromatic residues: reverse engineering of a dephospho-CoA kinase. *Protein Sci.* **30**, 1022–1034. (doi:10.1002/pro.4068)

78. Riddle DS, Santiago JV, Bray-Hall ST, Doshi N, Grantcharova VP, Yi Q, Baker D. 1997 Functional rapidly folding proteins from simplified amino acid sequences. *Nat. Struct. Biol.* **4**, 805–809. (doi:10.1038/nsb1097-805)

79. Kimura M, Akanuma S. 2020 Reconstruction and characterization of thermally stable and catalytically active proteins comprising an alphabet of ∼13 amino acids. *J. Mol. Evol.* **88**, 372–381. (doi:10.1007/s00239-020-09938-0)

80. Longo LM, Tenorio CA, Kumru OS, Middaugh CR, Blaber M. 2015 A single aromatic core mutation converts a designed 'primitive' protein from halophile to mesophile folding. *Protein Sci.* **24**, 27–37. (doi:10.1002/pro.2580)

81. Yagi S, Padhi AK, Vucinic J, Barbe S, Schiex T, Nakagawa R, Simoncini D, Zhang KYJ, Tagami S. 2021 Seven amino acid types suffice to create the core fold of RNA polymerase. *J. Am. Chem. Soc.* **143**, 15 998–16 006. (doi:10.1021/jacs.1c05367)

82. Foden CS, Islam S, Fernández-García C, Maugeri L, Sheppard TD, Powner MW. 2020 Prebiotic synthesis of cysteine peptides that catalyze peptide ligation in neutral water. *Science* **370**, 865–869. (doi:10.1126/science.abd5680)

83. Miller SL. 1953 A production of amino acids under possible primitive earth conditions. *Science* **117**, 528–529. (doi:10.1126/science.117.3046.528)

84. Miller SL, Urey HC. 1959 Organic compound synthesis on the primitive earth. *Science* **130**, 245–251. (doi:10.1126/science.130.3370.245)

85. Parker ET, Cleaves HJ, Dworkin JP, Glavin DP, Callahan M, Aubrey A, Lazcano A, Bada JL. 2011 Primordial synthesis of amines and amino acids in a 1958 Miller H_2S-rich spark discharge experiment. *Proc. Natl Acad. Sci. USA* **108**, 5526–5531. (doi:10.1073/pnas.1019191108)

86. Johnson AP, James Cleaves H, Dworkin JP, Glavin DP, Lazcano A, Bada JL. 2008 The Miller volcanic spark discharge experiment. *Science* **322**, 404–404. (doi:10.1126/science.1161527)

87. Cronin JR, Pizzarello S. 1983 Amino acids in meteorites. *Adv. Space Res.* **3**, 5–18. (doi:10.1016/0273-1177(83)90036-4)

88. Glavin DP, Elsila JE, McLain HL, Aponte JC, Parker ET, Dworkin JP, Hill DH, Connolly Jr HC, Lauretta DS. 2021 Extraterrestrial amino acids and L-enantiomeric excesses in the CM2 carbonaceous chondrites Aguas Zarcas and Murchison. *Meteorit. Planet. Sci.* **56**, 148–173. (doi:10.1111/maps.13451)

89. Kebukawa Y, Asano S, Tani A, Yoda I, Kobayashi K. 2022 Gamma-ray-induced amino acid formation in aqueous small bodies in the early solar system. *ACS Central Sci.* **8**, 1664–1671. (doi:10.1021/acscentsci.2c00588)

90. Holden DT, Morato NM, Cooks RG. 2022 Aqueous microdroplets enable abiotic synthesis and chain extension of unique peptide isomers from free amino acids. *Proc. Natl Acad. Sci. USA* **119**, e2212642119. (doi:10.1073/pnas.2212642119)

91. Griffith EC, Vaida V. 2012 In situ observation of peptide bond formation at the water–air interface. *Proc. Natl Acad. Sci. USA* **109**, 15 697–15 701. (doi:10.1073/pnas.1210029109)

92. Deal AM, Rapf RJ, Vaida V. 2021 Water–air interfaces as environments to address the water paradox in prebiotic chemistry: a physical chemistry perspective. *J. Phys. Chem. A* **125**, 4929–4942. (doi:10.1021/acs.jpca.1c02864)

93. Furukawa Y, Otake T, Ishiguro T, Nakazawa H, Kakegawa T. 2012 Abiotic formation of valine peptides under conditions of high temperature and high pressure. *Orig. Life Evol. Biosph.* **42**, 519–531. (doi:10.1007/s11084-012-9295-0)

94. Lambert JF. 2008 Adsorption and polymerization of amino acids on mineral surfaces: a review. *Orig. Life Evol. Biosph.* **38**, 211–242. (doi:10.1007/s11084-008-9128-3)

95. Takahagi W *et al.* 2019 Peptide synthesis under the alkaline hydrothermal conditions on Enceladus. *ACS Earth Space Chem.* **3**, 2559–2568. (doi:10.1021/acsearthspacechem.9b00108)

96. Kitadai N, Maruyama S. 2018 Origins of building blocks of life: a review. *Geosci. Front.* **9**, 1117–1153. (doi:10.1016/j.gsf.2017.07.007)

97. Flory PJ. 1953 *Principles of polymer chemistry*. Ithaca, NY: Cornell University Press.

98. Rollins GC, Dill KA. 2014 General mechanism of two-state protein folding kinetics. *J. Am. Chem. Soc.* **136**, 11 420–11 427. (doi:10.1021/ja5049434)

99. Frenkel-Pinter M *et al.* 2020 Mutually stabilizing interactions between proto-peptides and RNA. *Nat. Commun.* **11**, 3137. (doi:10.1038/s41467-020-16891-5)

100. Bose T *et al.* 2022 Origin of life: protoribosome forms peptide bonds and links RNA and protein dominated worlds. *Nucl. Acids Res.* **50**, 1815–1828. (doi:10.1093/nar/gkac052)

101. Tilman D. 1982 *Resource competition and community structure*. Princeton, NJ: Princeton University Press.

102. MacArthur R. 1970 Species packing and competitive equilibrium for many species. *Theor. Popul. Biol.* **1**, 1–11. (doi:10.1016/0040-5809(70)90039-0)